

Raman scattering study of SbSBr at high pressure

M. K. Teng, J. F. Vittori, and M. Massot

Laboratoire de Physique des Solides, Université Pierre et Marie Curie, T13 E2, 4 place Jussieu, F-75252 Paris CEDEX 05, France

S. Ziolkewicz

Laboratoire d'Ultrasons, Université Pierre et Marie Curie, T13 E1, 4 place Jussieu, F-75252 Paris CEDEX 05, France

A. Polian

Physique des Milieux Condensés, Université Pierre et Marie Curie, T13 E4, 4 place Jussieu, F-75252 Paris CEDEX 05, France

(Received 13 May 1988; revised manuscript received 11 October 1988)

The vibrational properties of the quasi-one-dimensional crystal SbSBr have been studied by Raman scattering as a function of pressure up to 21 GPa. Compressibilities parallel and perpendicular to the chain axis were measured by a microphotographic technique. This pressure study on one-dimensional crystals shows the very high stability of this structure. It also shows that the high-pressure behavior of the modes helps in the identification of the modes symmetry.

I. INTRODUCTION

Antimony sulfobromide SbSBr belongs to the V-VI-VII family, which has been intensively studied during the last three decades.¹⁻¹⁰ At room temperature and zero pressure it has the same orthorhombic structure $Pnam$ (D_{2h}^{16}) as antimony sulfoiodide and, like this crystal, has a chain-like one-dimensional (1D) structure. Its crystallographic parameters at ambient conditions are $a = 8.26 \text{ \AA}$, $b = 9.79 \text{ \AA}$, and $c = 3.97 \text{ \AA}$.¹¹ This family of crystals is known to undergo a displacive ferroelectric phase transition at low temperature;^{12,13} the transition temperature of SbSBr, still being controversial,^{1,5,14,15} is between 22.8 and 90 K.

In the paraelectric phase, SbSBr crystallizes in the D_{2h}^{16} space group and in the C_{2v}^2 space group in the ferroelectric phase. In both phases, there are four formula units per unit cell, leading to 36 normal modes out of which 18 are Raman active in the paraelectric phase and 33 in the ferroelectric phase.

In this paper, we will be concerned only with the high-temperature paraelectric phase. In this structure (Fig. 1) two formula units are strongly bound and form the central chain, which is weakly bound by van der Waals interaction to the other two. It was tempting then to describe the vibrational properties of this class of crystals using a simplified unit cell (C_{2h}^2 space group) containing only the central chain. In this description, there are only six atoms in the unit cell and thus 18 normal modes, nine of them being Raman active.¹⁶ Table I shows the correlations between the symmetry of the normal modes in these two structures, together with the corresponding activities (Raman, infrared, or silent) of the modes. The (formal) change from the one-chain to the two-chain description results in a folding of the Brillouin zone in a direction

perpendicular to the c axis, similar to the Brillouin-zone folding in the layer compound GaSe, when one goes from a one-layer polytype (γ) to a two-layer polytype (ϵ) and again to a four-layer polytype (δ).¹⁷ Such a description of SbSI-type crystals results in the apparition of Davydov

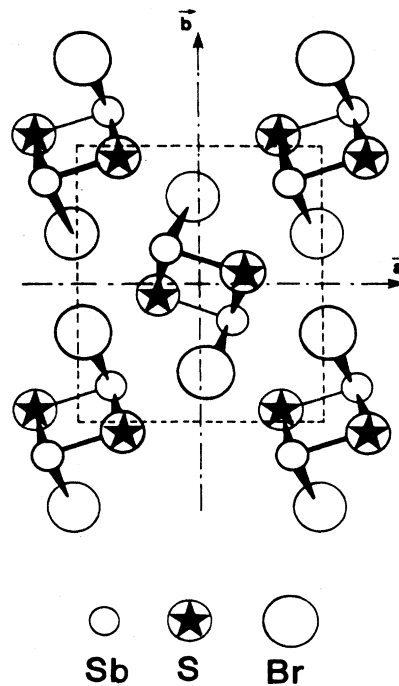


FIG. 1. Structure of SbSBr perpendicular to the c axis. The upper atoms are at a position $\frac{3}{4}$ in units of c and the lower ones at $\frac{1}{4}$.

TABLE I. Correlation chart between the D_{2h}^{16} and the C_{2h}^2 space groups. Representations are given with the corresponding activities: *R*, Raman; *ir*, infrared; *ac*, acoustical; *S*, silent.

D_{2h}^{16}	C_{2h}^2
6 A_g (R)	6 A_g (R)
6 B_{1g} (R)	6 A_g (R)
3 B_{2g} (R)	3 B_g (R)
3 B_{3g} (R)	3 B_g (R)
2 B_{1u} (<i>ir</i>)	2 A_u (<i>ir</i>)
1 B_{1u} (<i>ac</i>)	1 A_u (<i>ac</i>)
3 A_u (<i>S</i>)	1 A_u (<i>ac</i>)
5 B_{2u} (<i>ir</i>)	4 B_u (<i>ir</i>)
1 B_{2u} (<i>ac</i>)	4 B_u (<i>ir</i>)
5 B_{3u} (<i>ir</i>)	2 B_u (<i>ac</i>)
1 B_{3u} (<i>ac</i>)	2 B_u (<i>ac</i>)

doublets, one component of which corresponds to the zone-center mode of the one-chain structure, the other one to the zone-edge mode. The Davydov conjugate of the acoustic modes will be "rigid-chain" modes, which correspond to the zone-edge acoustic phonons of the compound with one chain in the unit cell. Up to now, almost all the interpretations of the Raman studies and all the lattice dynamical models have been performed on the one-chain structure (C_{2h}^2 space group).^{14,16,18} This is the reason why there are still controversies in the attribution of the modes.

In a previous paper,⁸ zero-pressure Raman spectra of SbSBr were compared to those of SbSI, BiSI, SbSeI, and BiSeI. Furman *et al.*¹⁴ have investigated the Raman spectrum as a function of temperature through the ferroelectric phase transition, and as a function of the I-Br atomic substitution. More recently, Inushima *et al.*^{15,16} measured again the Raman spectra as a function of temperature, and their data were interpreted using lattice-dynamical calculations. In the latter experiment, soft-mode behavior was observed at the phase transition.

In this paper, we present the effect of pressure on the Raman spectrum of SbSBr. The pressure is a good thermodynamical parameter since it only varies the interatomic distances. In 1D crystals, the interchain space will take most of the compression, so the modes which are driven by the van der Waals interaction will be much more affected than the other ones, and thus will be distinguished by their pressure derivatives.

In Sec. II, we will briefly describe the experimental procedure to measure the compressibility and the Raman

spectra as a function of pressure in a diamond-anvil cell (DAC). The results will be presented in Sec. III and discussed in Sec. IV.

II. EXPERIMENTAL

The Raman-scattering experiments were carried out in the backscattering geometry using a triple-monochromator spectrometer and approximately 50 mW of the 676.4-nm line of a krypton laser.

The DAC was of the Block-Piermarini type.¹⁹ The pressure-transmitting medium was a 4:1 methanol-ethanol mixture and the pressure was measured using the linear ruby fluorescence scale with a pressure coefficient of $-7.56 \text{ cm}^{-1} \text{ GPa}^{-1}$.

SbSBr single crystals were grown by the vapor-transport method. Details of the crystal growth procedure are reported in Ref. 8. The samples used in the present experiments were needles $\approx 100 \mu\text{m}$ long and $\approx 20 \mu\text{m}$ thick, with the *c* axis perpendicular to the optical axis of the DAC.

Using the same geometry, the linear compressibilities parallel and perpendicular to the *c* axis were measured by a microphotographic technique.²⁰ In this set of experiments, it was not possible to differentiate the *a* and *b* axes so the compressibility is supposed isotropic perpendicular to the *c* axis.

III. RESULTS

Raman spectra were performed up to 21 GPa in the frequency range from 5 to 360 cm^{-1} . Because of the depolarization effects due to the stressed diamond anvils, polarization measurements were not performed. Moreover, the band gap of SbSBr shifts to lower energy under pressure, so the crystals become more and more opaque to the laser light and no Raman spectra were obtained above 21 GPa.

Figure 2 shows the complete spectrum at various pressures. Some features in these spectra can be pointed out.

(i) In the low-wave-number region of the spectrum, the intensity of the mode at 61.5 cm^{-1} at $P=0$ decreases with increasing pressure and the relevant phonon is not observable above 5 GPa.

(ii) The high-wave-number component of the doublet $78.5\text{--}82.5 \text{ cm}^{-1}$ at $P=0$ is not observable above 6 GPa.

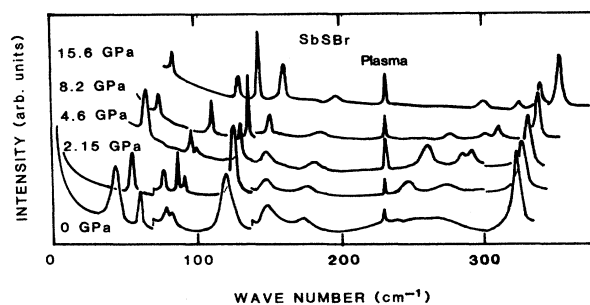


FIG. 2. Full Raman spectrum at various pressures showing the pressure dependence of the phonons.

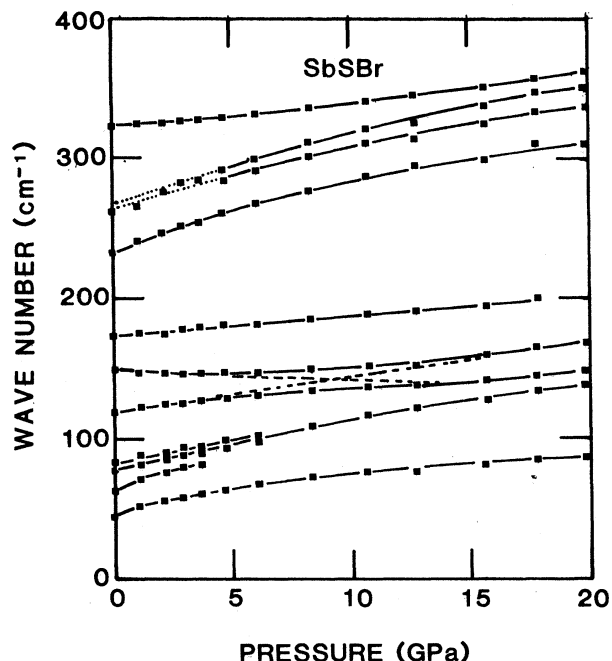


FIG. 3. Pressure dependence of the observed lines.

(iii) At room pressure a broad band between 200 and 300 cm^{-1} cannot be resolved into individual peaks. High pressure splits it into at least three separate components.

(iv) The width of several peaks decreases with increasing pressure and the wave number of the peak at 148.5 cm^{-1} ($P=0$) first decreases with pressure up to 5 GPa and then increases again.

The variation with pressure of the individual modes is summarized in Fig. 3 and Table II.

In order to compute the Grüneisen parameter of the modes, the compressibility is needed. The linear compressibilities parallel and perpendicular to the c axis were measured by the method described in the preceding section and the results are shown in Fig. 4. The mechanical anisotropy of this crystal is very strong since the initial compressibility parallel to the c axis is about 2 orders

TABLE II. Pressure coefficients of the observed Raman active modes.

Wave numbers at $P=0$ (cm^{-1})	Pressure coefficients $\frac{1}{\omega} \left[\frac{\partial \omega}{\partial P} \right]$ (10^{-3} GPa^{-1})
43.6	159
61.5	143
78.5	41
82.5	50
119	19
148.5	-12
173	8
232.5	25
264	16
266	20
322	4.3

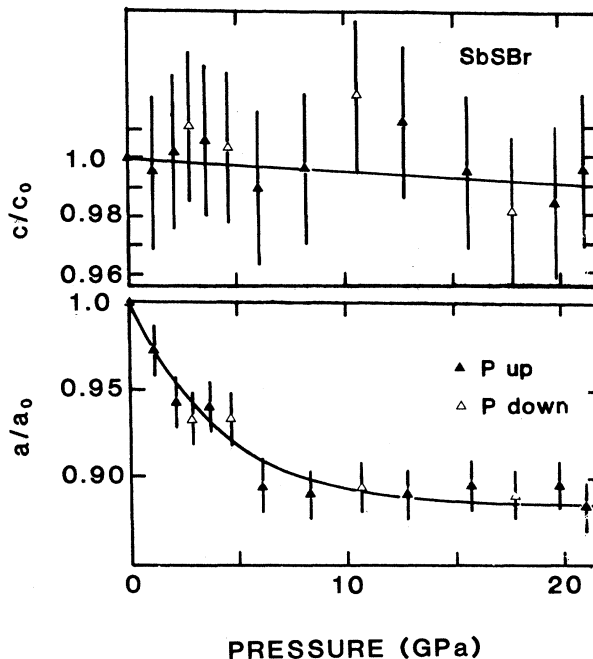


FIG. 4. Pressure dependence of the relative deformations of the chains. Points are obtained at increasing pressure, open circles at decreasing pressure. The lines are guides for the eye.

of magnitude smaller than that perpendicular to c . Moreover, for pressures above ≈ 10 GPa, the linear compressibilities parallel and perpendicular to the c axis have the same value, i.e., the crystal become more isotropic when pressure is applied.²¹

The room-pressure compressibilities are

$$-\frac{1}{c} \left[\frac{\partial c}{\partial P} \right]_T \approx 4.5 \times 10^{-4} \text{ GPa}^{-1},$$

$$-\frac{1}{a} \left[\frac{\partial a}{\partial P} \right]_T \approx 2.5 \times 10^{-2} \text{ GPa}^{-1}.$$

IV. DISCUSSION

As in all low-dimensional crystals, the differences in interatomic forces is expressed by the large anisotropy of the linear compressibilities perpendicular (van der Waals forces) and parallel (ionico-covalent forces) to the chain axis. The pressure dependence of the compressibilities is also characteristic of low-dimensional crystals: the compressibility of the strongly bonded molecular units (intrachain in 1D crystals, intralayer in 2D crystals) is almost pressure independent, whereas the compressibility of the intermolecular space, which is very large at ambient conditions, decreases very rapidly under pressure. The high-pressure values of both linear compressibilities are of the same order of magnitude. This change of the relative magnitude of the intramolecular and intermolecular restoring forces does not bring about any phase transformation and, on the contrary, shows the remarkably high stability of these compounds.

The consequence of this behavior for the lattice modes is that, at low pressure, one should be able to easily discriminate the phonons whose frequency depends mainly on the interchain interactions from those depending on the intrachain interactions.²² This can be viewed in Fig. 3. Considering the pressure dependence of the modes, it is to be seen that two are interchain modes: $\sigma = 43.5$ and 61.5 cm^{-1} at $P=0$, whereas the others are mainly intrachain modes. The pressure coefficients of the modes are also summed up in Table II, where it is to be seen that the two low-wave-number modes have pressure coefficients about 1 order of magnitude larger than that of the other modes.

Some features should be discussed here.

(i) The intensity of the low-wave-number mode ($\sigma = 60 \text{ cm}^{-1}$ at $P=0$) decreases regularly with pressure. This fact may be related to the pressure dependence of the polarizability of the bonds involved in this phonon.

(ii) The two components of the doublet at 78.5 and 82.5 cm^{-1} at $P=0$ both assigned by Inushima *et al.*¹⁶ to B_{1g} are parallel when plotted as a function of pressure (Fig. 3). Such behavior may only be understood if the restoring forces involved in both modes are almost the same. Unfortunately, no lattice-dynamical model^{16,23} shows the displacement pattern for these modes.

(iii) The two modes at 119 and 148.5 cm^{-1} at $P=0$ show an anticrossing around 10 GPa . The upper mode has a negative pressure coefficient [see point (iv)] whereas the lower mode has a positive one. These two modes are assigned as A_g . The fact that they repel each other confirms the assignment of both modes to the same symmetry.

(iv) The pressure behavior of the mode at 148.5 cm^{-1} at $P=0$ is surprising: at low pressure its initial slope is negative. Such behavior can correspond either to an increase of interatomic distances or to a weakening of the restoring forces. If the attribution is right, this mode is A_g^4 ,¹⁶ where the bromine atoms are almost at rest and the other atoms of the central chain move like a deformable tetrahedron with rigid arms. If the interatomic distances were increasing with pressure, this would certainly affect other modes, so one can infer that the displacement pattern of this mode destabilizes the structure, and so the frequency decreases down to the point where the A_g^4 mode interacts with the A_g^3 mode.

(v) Between 200 and 300 cm^{-1} , the room-pressure spectrum shows a broad band which cannot be resolved, even at low temperature.¹⁶ On the other hand, the application of pressure shows that there are at least three peaks hidden in this band. One of them can be extrapolated at 232 cm^{-1} and the other two at approximately 264 and 266 cm^{-1} at $P=0$. It is naturally difficult to determine the symmetry of these modes; nevertheless, it is to be seen in Fig. 3 that the slope of the mode at 322 cm^{-1} ($P=0$) which is unambiguously A_g (Refs. 14 and 16) increases when the mode at 266 cm^{-1} comes closer, so it should also be A_g .

It is not necessary to put forward any phase transformation to explain these properties because the relative intensity of the modes evolves continuously with pressure.

Finally, the complete set of modes observed by the

TABLE III. Recapitulation of the Raman modes observed by various authors.

$\sigma \text{ (cm}^{-1}\text{)}$	Symmetry C_{2h}	Symmetry D_{2h}^b
43.5	$B_g^{a,c}$	B_{2g} or B_{3g}
47	A_g^b	A_g
61.5	$A_g^{a,c}$	A_g
78.5	$A_g^{a,c}$	B_{1g}
82.5	B_g^c	B_{1g}
119	$A_g^{a,c}$	A_g
136	A_g^a	B_{1g}
148.5	$A_g^{a,c}$	A_g
173	$A_g^a - B_g^c$	B_{1g}
217		B_{2g} or B_{3g}
225	B_g^a	
232.5	B_g^c	
264	A_g or B_g^a	
266	A_g^c	
315	A_g^a	
322	$A_g^{a,c}$	

^aReference 14.

^bReference 16.

^cPresent work.

various groups is shown in Table III, with the attributions of Furman *et al.*,¹⁴ Inushima *et al.*,¹⁶ and the present work. One point is very striking in view of this table: there are only nine modes which are observed by at least two groups. This is a very strong indication that in SbSBr, as in all the low-dimensional crystals, crystalline imperfections play an important role. It shows that the C_{2h}^2 space-group description is almost valid for the room-pressure studies; the other modes allowed in the D_{2h}^{16} structure may be activated by imperfections. Nevertheless, from the 18 Raman-active modes of the D_{2h}^{16} structure, 16 have been observed by at least one group.

V. CONCLUSION

The chainlike crystal SbSBr has been studied by Raman spectroscopy under high pressure, the compressibility being determined by a microphotographic technique. The main result of this study is the very high stability of this low-dimensional compound under pressure, stability which was already established for the layered compounds. The present result shows that pressure is a parameter which helps to identify the symmetry of the modes. It also shows that the reduced space-group description is good under normal conditions, even if the true one is D_{2h}^{16} . From the 18 Raman-allowed modes, only two were never observed.

ACKNOWLEDGMENT

Critical reading of the manuscript by J. M. Besson is kindly acknowledged. Laboratoire de Physique des Solides is unité associée au Centre National de la Recherche Scientifique No. 154. Laboratoire d'Ultrasons is unité associée au Centre National de la Recherche Scientifique No. 789. Physique des Milieux Condensés is unité associée au Centre National de la Recherche Scientifique No. 782.

- ¹R. Nitsche, H. Roetzsch, and P. Wild, *Appl. Phys. Lett.* **4**, 210 (1964).
- ²T. Mori, H. Tamura, and E. Sawaguchi, *J. Phys. Soc. Jpn. (Suppl.)* **28**, 445 (1970).
- ³G. Harbeke, *J. Phys. Chem. Solids* **24**, 957 (1963).
- ⁴M. K. Teng, M. Balkanski, and M. Massot, *Phys. Rev. B* **5**, 1031 (1972).
- ⁵T. A. Pikka and V. M. Fridkin, *Fiz. Tverd. Tela (Leningrad)* **10**, 3378 (1968) [*Sov. Phys.—Solid State* **10**, 2668 (1969)].
- ⁶G. A. Samara, *Phys. Lett. A* **27**, 232 (1968).
- ⁷P. S. Peercy, *Phys. Rev. Lett.* **35**, 1581 (1975).
- ⁸M. K. Teng, M. Balkanski, M. Massot, and S. Ziolkiewicz, *Phys. Status Solidi* **62**, 173 (1974).
- ⁹R. Blinc, M. Mali, and A. Novak, *Solid State Commun.* **6**, 327 (1968).
- ¹⁰J. Petzelt, *Phys. Status Solidi* **36**, 321 (1969).
- ¹¹E. Donges, *Z. Anorg. Allg. Chem.* **263**, 112 (1950).
- ¹²A. Kikuchi, Y. Oka, and E. Sawaguchi, *J. Phys. Soc. Jpn.* **23**, 337 (1967).
- ¹³T. Takama and T. Mitsui, *J. Phys. Soc. Jpn.* **23**, 331 (1967).
- ¹⁴E. Furman, O. Brafman, and J. Makovsky, *Phys. Rev. B* **8**, 2341 (1973).
- ¹⁵T. Inushima, A. Okamoto, K. Uchinokura, and E. Matsuura, *J. Phys. Soc. Jpn.* **48**, 2167 (1980).
- ¹⁶T. Inushima, K. Uchinokura, K. Sasahara, and E. Matsuura, *Phys. Rev. B* **26**, 2525 (1982).
- ¹⁷A. Polian, K. Kunc, and A. Kuhn, *Solid State Commun.* **19**, 1079 (1976).
- ¹⁸M. Balkanski, M. K. Teng, S. M. Shapiro, and S. Ziolkiewicz, *Phys. Status Solidi* **44**, 355 (1971).
- ¹⁹G. J. Piermarini, S. Block, J. D. Barnett, and R. A. Forman, *J. Appl. Phys.* **46**, 2774 (1975).
- ²⁰A. Polian, J. M. Besson, M. Grimsditch, and H. Vogt, *Phys. Rev. B* **25**, 2767 (1982).
- ²¹M. Gauthier, A. Polian, J. M. Besson, and A. Chevy (unpublished).
- ²²R. Zallen, *Phys. Rev. B* **9**, 4485 (1974).
- ²³E. Furman, O. Brafman, and J. Makovski, *Phys. Rev. B* **13**, 1703 (1976).